

NOTE

Yoshitaka Kubojima · Hideo Kato · Mario Tonosaki

Proportional limit of wood obtained from a load–time diagram during an impact bending test

Received: September 28, 2001 / Accepted: January 9, 2002

Abstract We transferred the linear part of a load–deflection diagram from an impact bending test of wood into a load–time diagram. In addition, we proposed a method to obtain the proportional limit from the load–time diagram. Japanese cedar (*Cryptomeria japonica* D. Don), hondo spruce (*Picea yezoensis* Carr. var. *hondoensis* Rehd.), hiba arbor-vitae (*Thujaopsis dolabrata* Sieb. et Zucc.), Japanese red pine (*Pinus densiflora* Sieb. et Zucc.), paulownia (*Paulownia tomentosa* Steud.), Manchurian ash (*Fraxinus mandshurica* Rupr.), and Japanese evergreen oak (*Quercus acuta* Thunb.) were used in this study. The dimensions of each specimen were 115mm (L) × 7mm (R) × 7mm (T). The results were as follows: (1) The linear region of the load–deflection diagram in the impact bending test could be transferred with sufficient accuracy to a load–time diagram using a sine function. (2) Approximating the load–time diagram by a linear equation was useful for obtaining the proportional limit.

Key words Proportional limit · Impact bending test · Load–deflection diagram · Load–time diagram · Sine function

Introduction

When wood is used as structural lumber, toughness (as well as stiffness and strength) is extremely important. When measuring the toughness of wood, bending tests are frequently used to obtain Young's modulus, proportional limit, strength, and absorbed energy.

To investigate absorbed energies during static or impact bending in detail, the load–deflection and load–time diagrams are divided into several parts, such as an elastic

region, a plastic region, and a region after rupture.^{1–4} Factors that contributed to the total absorbed energy can be estimated using this method.

Load is measured with a load cell of a measuring machine for the static bending test; and for the impact bending test it is expressed as the product of acceleration measured with an acceleration transducer attached to a hammer of a measuring system multiplied by the mass of the hammer. The deformation of a specimen during bending tests can be obtained from the movement of a crosshead in the static bending test and from a strain-gauge bonded to a specimen in the impact bending test.

To investigate the entire process of the bending tests, measurements must be taken before and after rupture. However, for the impact bending test, the strain-gauge is often read inaccurately during the deformation of a specimen. When a strain-gauge is broken, the strain is infinity; but when two wires of a strain-gauge come into contact with each other, the circuit containing the strain-gauge is shorted and shows a strain value of 0. Although the load–time diagram can be recorded through the entire process of the impact bending test, the proportional limit of the load–deflection diagram cannot be determined directly from the load–time diagram.

In this study, we transcribed the linear part of the load–deflection diagram during an impact bending test of wood into a load–time diagram. In addition, we devised a method to obtain the proportional limit from the load–time diagram.

Theory

The horizontal motion of a hammer of an impact bending machine is investigated. The hammer is subject to the reaction (F) from a specimen. The movement of the hammer is equal to the bend of a specimen (y). Therefore, in a linear region of a load–deflection diagram:

$$F = -Ay \quad (1)$$

Y. Kubojima (✉) · H. Kato · M. Tonosaki
Forestry and Forest Products Research Institute, PO Box 16,
Tsukuba Norin Kenkyu Danchi-nai, Ibaraki 305-8687, Japan
Tel. +81-298-73-3211; Fax +81-298-74-3720
e-mail: kubojima@ffpri.affrc.go.jp

where A is a constant.

$$\therefore m \frac{d^2 y}{dt^2} = -Ay \quad (2)$$

where m is the mass of a hammer, and t is time.

$$\therefore y = B \sin\left(\sqrt{\frac{A}{m}} t\right) (y = 0 \text{ at } t = 0) \quad (3)$$

where B is a constant. Then, assuming $v = v_0$ (v is velocity) at $t = 0$,

$$F = -\sqrt{Am}v_0 \sin\left(\sqrt{\frac{A}{m}} t\right) \quad (4)$$

Here, A is expressed using width b , thickness h , length l , and Young's modulus E of a specimen with a rectangular cross section as follows.

$$A = \frac{4bh^3}{l^3} E \quad (5)$$

In this study, stress (σ) and strain (ε) in the axial direction were used instead of F and y , respectively, where

$$\sigma = \frac{3l}{2bh^3} F \quad (7)$$

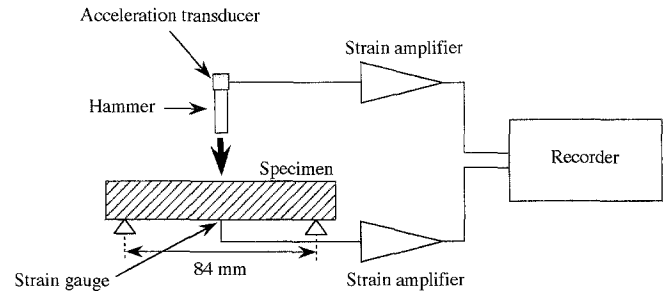


Fig. 1. Impact bending tester

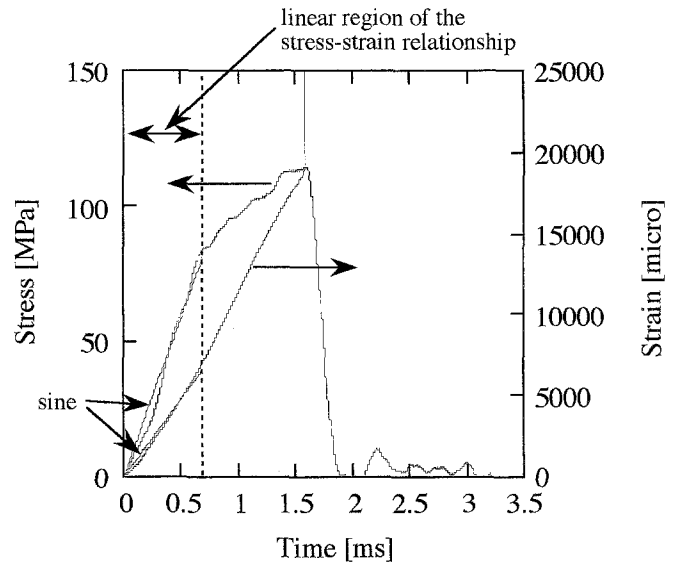


Fig. 2. Stress–time and strain–time diagrams (hiba). The linear region of the stress–strain diagram in Fig. 3 was approximated by a sine function

Experimental

Specimens

Sugi (Japanese cedar; *Cryptomeria japonica* D. Don), tohi (hondo spruce; *Picea yezoensis* Carr. var. *hondoensis* Rehd.), hiba (hiba arbor-vitae; *Thujopsis dolabrata* Sieb. et Zucc.), akamatsu (Japanese red pine; *Pinus densiflora* Sieb. et Zucc.), kiri (paulownia; *Paulownia tomentosa* Steud.), yachidamo (Manchurian ash; *Fraxinus mandshurica* Rupr.), and akagashi (Japanese evergreen oak; *Quercus acuta* Thunb.) were used. The dimensions of each specimen were 115 mm (L) \times 7 mm (R) \times 7 mm (T). Five specimens from each species were used. The specimens were conditioned at 20°C and 65% relative humidity. The tests were conducted under the same conditions.

Impact bending test

Figure 1 shows the equipment for the impact bending test. A Charpy-type impact bending machine with a capacity of 30 kgw·cm (Charpy-type impact bending machine 4002; Mori Testing Machine Co.) was used. The span was 84 mm. To obtain information on fracture mechanisms, an acceleration transducer with a capacity of 50 G ($G = 9.81 \text{ m/s}^2$) (acceleration transducer AS-50HB; Kyowa Electronic Instruments) was attached to a hammer of the machine and a strain-gauge (FLA-2-11; Tokyo Sokki Kenkyujo) was

bonded to the surface of the tensioned plane of the specimen. The outputs from the transducer and strain-gauge were amplified and recorded (DC-92D, Tokyo Sokki Kenkyujo; APC-204, Autonics).⁵ Load (product of the mass of the hammer and the acceleration)–time and strain–time diagrams were then obtained. The load and the strain were recorded as digital data at intervals of 1 μs .

Results and discussion

Figure 2 shows the stress–time and strain–time diagrams. The infinite value of the strain means that the strain-gauge was broken at the moment of rupture.

To investigate the proportional limit, appropriate linear regions must be measured. If an appropriate linear region appears, it should be possible to obtain an adequate Young's modulus. Thus, Young's modulus is used as an index to indicate whether experiments were done accurately.

A stress–strain diagram is shown in Fig. 3 using the data shown in Fig. 2. The linear region was determined as follows: Choosing a value of stress ($\sigma_{\pm 0}$) that was thought to be

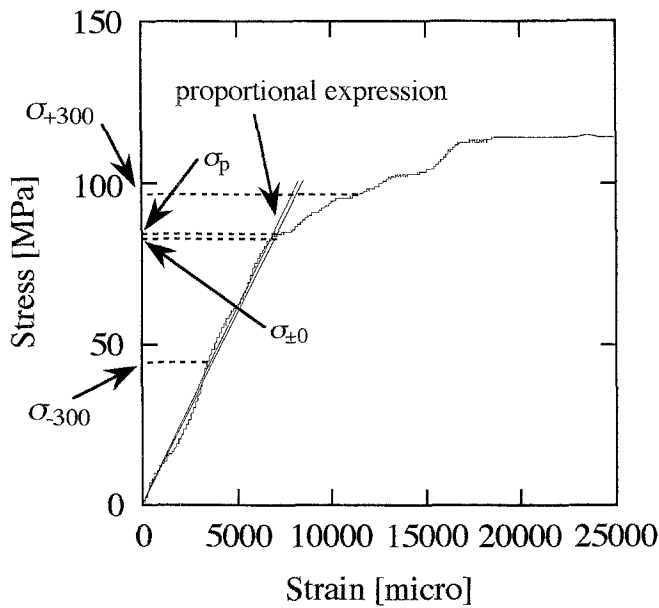


Fig. 3. Stress-strain diagram (hiba). Values are from Fig. 2

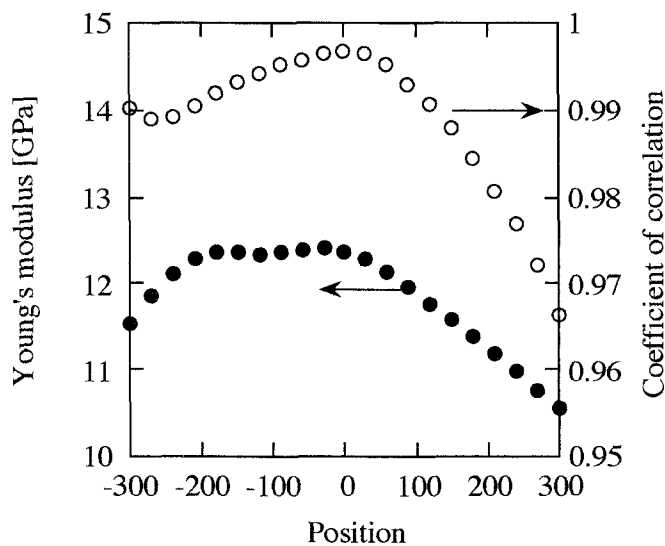


Fig. 4. Changes in Young's modulus and the coefficient of correlation (hiba). Position means the distance in point numbers between $\sigma_{\pm 0}$ and each upper limit of the approximating region

the point corresponding to the start of nonlinearity, the range from $\sigma = 0$ to values around $\sigma_{\pm 0}$ were approximated by a proportional expression; in other words, data in regions of $0 \leq \sigma \leq \sigma_{-300}$, $0 \leq \sigma \leq \sigma_{-270}$, \dots , $0 \leq \sigma \leq \sigma_{-60}$, $0 \leq \sigma \leq \sigma_{-30}$, $0 \leq \sigma \leq \sigma_{\pm 0}$, $0 \leq \sigma \leq \sigma_{+30}$, $0 \leq \sigma \leq \sigma_{+60}$, \dots , $0 \leq \sigma \leq \sigma_{+270}$, and $0 \leq \sigma \leq \sigma_{+300}$ were approximated by a proportional expression (Fig. 3). For example, the subscripts -30 and $+30$ represent the values of 30 points before and after $\sigma_{\pm 0}$, respectively.

Young's modulus (the slope of the line) and the coefficient of correlation obtained by approximation using the proportional expression are plotted against the position that corresponds to each upper limit of σ in the approximating region, as in Fig. 4. If $\sigma_{\pm 0}$ is equal to the point corresponding to the start of nonlinearity, Young's modulus

and the coefficient of correlation theoretically must have the following tendencies: Both Young's modulus and the coefficient of correlation are constant (in the case of the coefficient of correlation, the constant value is 1) if the upper limit is $\leq \sigma_{\pm 0}$. When an upper limit $> \sigma_{\pm 0}$ is contained in the approximating region, both Young's modulus and the coefficient of correlation decrease monotonically with the position. Generally speaking, the results in Fig. 4 were as expected. It is understood that there is a linear region and a curved one in the load-deflection diagram, and the boundary between the linear and curved regions could be determined clearly by this impact bending test. The smaller Young's modulus and coefficient of correlation appearing at the narrower approximating region were influenced by the irregular results at the starting point of the stress-strain diagram.

Young's modulus from the impact bending test is shown in Table 1. Comparing Young's modulus in this study to Young's modulus in static bending,⁶ the Young's modulus obtained from this impact bending test is thought to be adequate.

Given that the boundary between the linear and curved parts was clear in the load-deflection diagram and that Young's modulus was proper, this impact bending test was carried out appropriately. Therefore, we believe that $\sigma_{\pm 0}$ nearly is equal to the point corresponding to the start of nonlinearity. A proportional limit of 3% (σ_p) was used in this study.

The stress-time and strain-time diagrams corresponding to the linear region of the stress-strain diagram shown in Fig. 3 are approximated by a sine function, as shown in Fig. 2: $\sigma = a_1 \sin b_1 t$ and $\varepsilon = a_2 \sin b_2 t$ (where a_1 , a_2 , b_1 , and b_2 are constants). The coefficients of correlation listed in Table 1 confirmed experimentally that stress and strain were expressed by sine functions. In addition, the result of $b_1/b_2 \approx 1$ means that stress was proportional to strain. Calculating a_1/a_2 , it was similar to the Young's modulus obtained from the stress-strain diagram. Therefore, it is concluded that the linear region of the load-deflection diagram for the impact bending test can be transferred to the load-time diagram with sufficient accuracy using a sine function.

At the initial stage of the stress-time and strain-time diagrams, the experimental results were less than the calculated values. It is thought that this was caused by local compression by the hammer striking a specimen or idling of the measuring system.

Next, we investigated the accuracy of the proportional limit obtained from the load-time diagram from the impact bending test. The following assumes measurement of the proportional limit only by the load-time diagram without bonding a strain-gauge to a specimen.

The stress-time data shown in Fig. 5 were approximated by a sine function. Ideally, the coefficient of correlation is 1 in the range of $0 \leq \sigma \leq \sigma_p$ (σ_p is the proportional limit from the stress-strain diagram), and it decreases monotonically with the upper limit if the upper limit is larger than σ_p . However, the overall result was not as expected; for example, the coefficient of correlation in the range of $0 \leq \sigma \leq \sigma_{\max}$ (σ_{\max} is the maximum stress during rupture) was larger

Table 1. Results of the impact bending test when both stress and strain were measured

Wood	Coefficient of correlation		b_1/b_2	$(a_1/a_2)/E$	E (GPa)
	Stress	Strain			
Cedar	0.983	0.992	1.07	0.93	5.8
Spruce	0.982	0.994	0.93	1.08	10.8
Hiba	0.983	0.988	0.97	1.04	13.0
Pine	0.974	0.990	0.96	1.04	12.5
Paulownia	0.990	0.996	1.03	0.99	6.6
Ash	0.980	0.993	1.02	0.98	16.5
Oak	0.979	0.990	1.04	0.96	14.1

Values are the average for five specimens from each species. Stress and strain were approximated by $\sigma = a_1 \sin b_1 t$ and $\varepsilon = a_2 \sin b_2 t$, where a_1 , a_2 , b_1 , and b_2 are constants. E is Young's modulus from the stress-strain diagram

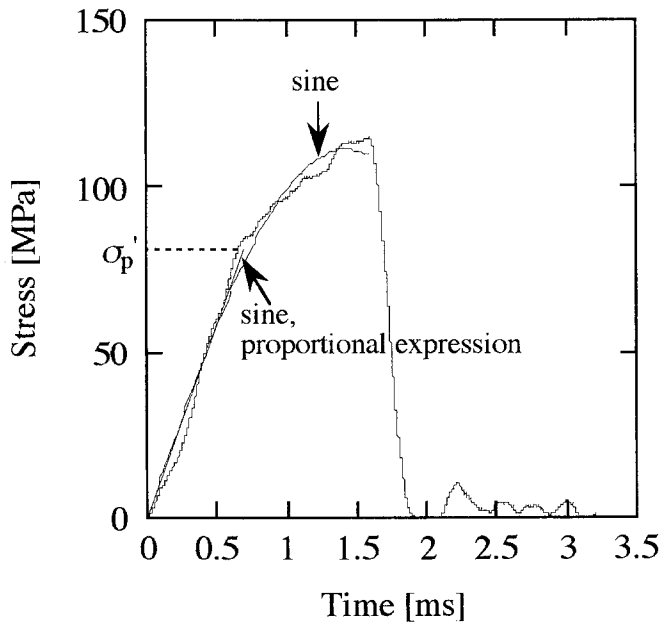


Fig. 5. Determination of the proportional limit from the load-time diagram (hiba). When stress in the range of $0 \leq \sigma \leq \sigma_p'$ was approximated by the sine function and the proportional expression, the results overlapped

than that in the range of $0 \leq \sigma \leq \sigma_p$ (Table 2). This tendency occurred because σ values larger than σ_p fit the sine function coincidentally. This result indicates that the coefficient of correlation of $0 \leq \sigma \leq \sigma_p$ is not always the largest value. Thus, it is not adequate to use a sine function to obtain the proportional limit experimentally from the load-time diagram.

Considering the shape of the stress-time graph, we tried approximation using a linear equation. The linear region was determined as follows: Choosing a stress value ($\sigma'_{\pm 0}$) that was thought to be the point corresponding to the start of nonlinearity, the range from $\sigma = 0$ to values around $\sigma'_{\pm 0}$ was approximated by a proportional expression. From the coefficient of correlation in Table 2, the stress could be expressed sufficiently by a linear equation. Comparing the 3% proportional limit by this method (σ_p') to that by the stress-strain diagram (σ_p), σ_p' was similar to σ_p . We think

Table 2. Determination of the proportional limit from the stress-time diagram

Wood	Coefficient of correlation		σ_p'/σ_p	
	Sine	Linear		
	$0 \leq \sigma \leq \sigma_p$	$0 \leq \sigma \leq \sigma_{\max}$		
Cedar	0.983	0.991	0.996	0.91
Spruce	0.982	0.991	0.996	0.99
Hiba	0.983	0.991	0.996	0.99
Pine	0.974	0.989	0.997	1.00
Paulownia	0.990	0.994	0.992	0.97
Ash	0.980	0.993	0.994	1.01
Oak	0.979	0.989	0.995	1.02

Values are the average for five specimens from each species. Stress is approximated by sine and linear equations. Coefficient of correlations of $0 \leq \sigma \leq \sigma_p$ are from Table 1

σ_{\max} , stress in rupture; σ_p , proportional limit from the stress-strain diagram; σ_p' , proportional limit obtained by approximating the stress-time diagram by a linear equation

that using the proportional limit obtained by approximating the load-time diagram as the proportional expression causes no problem when calculating the elastic and plastic works during impact bending.

Conclusion

We transferred the linear part of the load-deflection diagram to a load-time diagram for the impact bending test of wood and determined the proportional limit. Moreover, we proposed a simple method for obtaining the proportional limit from the load-time diagram using specimens from seven species with dimensions of 115 mm (L) \times 7 mm (R) \times 7 mm (T). Impact bending tests were conducted. The results were as follows: (1) The linear region of the load-deflection diagram during the impact bending test could be transferred to the load-time diagram with sufficient accuracy using a sine function. (2) Approximating the load-time diagram by a linear equation was useful for obtaining the proportional limit.

References

1. Liu Y, Nakayama Y, Kanagawa Y, Fujihara S (1999) Bending work of plantation grown Chinese fir (*Cunninghamia lanceolata* Hook.) (in Japanese). *Mokuzai Gakkaishi* 45:359–366
2. Kubojima Y, Okano T, Ohta M (2000) Bending strength and toughness of heat-treated wood. *J Wood Sci* 46:8–15
3. Kubojima Y, Ohsaki H, Sawada T, Origuchi K, Yoshihara H, Okano T (2000) Wood properties of sugi (*Cryptomeria japonica* D. Don) planted at Gobo-zawa in University Forest in Chiba (in Japanese). *Bull Tokyo Univ For* 103:243–306
4. Kollmann FFP, Côté WA Jr (1968) Principle of wood science and technology. Springer-Verlag, Berlin, pp 379–380
5. Ohta M, Asano I, Okano T (1979) Mechanical properties of brittleheart. II. Impact bending fracture (in Japanese). *Mokuzai Gakkaishi* 25:7–13
6. Government Forest Experiment Station (1958) Wood Industry Handbook (in Japanese). Maruzen, Tokyo, p 164